Renewable Energy 36 (2011) 2759–2770

Contents lists available at ScienceDirect

Renewable Energy

journal homepage: www.elsevier.com/locate/renene

Review

Optimal interface based on power electronics in distributed generation systems for fuel cells

J.M. Andújar [a], F. Segura [a,*], E. Durán [a], L.A. Rentería [b]

[a] Department of Electronic, Computer Science and Automatic Engineering, University of Huelva, Crta. Huelva-Palos de la Frontera s/n, 21819 Palos de la Frontera, Spain
[b] Department of Electronic Technology, Systems Engineering and Automatic, University of Cantabria, Avda. Los Castros s/n, 39005 Santander, Cantabria, Spain

ARTICLE INFO

Article history:
Received 23 December 2009
Accepted 7 April 2011
Available online 5 May 2011

Keywords:
Distributed generation (DG)
PEM fuel cell
Power electronics
Voltage control loop
PWM

ABSTRACT

A hybrid system comprising a fuel cell stack and a battery bank was developed, built and tested in this research work. This hybrid system was built to supply both DC and AC outputs. The voltage levels set on electrical interconnection points are achieved with several power conditioning stages controlled by Pulse Width Modulation (PWM). The main advantage of this system is its excellence as a test bench, since it allows testing system performance at different voltage-restricted interconnecting points. Besides, power electronics are observed to play an essential role in distributed generation systems. The applications of the developed hybrid system extend from Auxiliary Power Units (APU) in vehicles (cars, buses or trains) to Uninterruptible Power Systems (UPS) in hospitals, nursing homes, hotels, office buildings or schools.

1. Introduction

The aim of this paper is to present and explain the process to build and test an eco-friendly stand-alone system (no harmful emissions, noise or grid connection). The development, construction and real behavior of a stand-alone hybrid system are thus analyzed (Fig. 1). This system comprises a PEM fuel cell stack, a battery bank, four power converters and associated electronics. This hybrid system was sized to supply up to 1.5 kW and its outputs are 12 V-DC and 230 V–50 Hz-AC. DC and AC outputs make the hybrid system connection shown in Fig. 1 different from the systems studied in other works, since sources are connected to a low voltage DC Bus (48 V). Next, to obtain AC output, low voltage is converted into high voltage by a DC/DC converter (360 V) and a single-phase inverter generates AC output (220 V–50 Hz). On the other hand, a step-down DC/DC converter provides 12 V-DC. Voltage control loops are based on the PWM technique. One of the main advantages of this system is its excellence as a test bench, since it allows testing system performance at different voltage-restricted interconnecting points; besides, different load profiles can be applied. On the other hand, power electronics are observed to play an essential role in distributed generation systems [1,2].

Fuel cells are widely recognized as one of the most promising technologies to meet future power generation requirements, thus responding to concerns about oil consumption and dangerous CO_2 gas emissions [3,4]. One of their main advantages is their modularity, as they can be configured to operate within a wide range of output power: from 50 W to 50 MW. However, fuel cell dynamics is limited by the hydrogen/oxygen delivery system [5]. An auxiliary power source with a fast response therefore becomes necessary. Then, a combination of a fuel cell and a battery or ultracapacitor bank can form an ideal hybrid system [6]. Fuel cell hybrid systems applied to automotive, uninterruptible supply systems or auxiliary power systems have recently been researched [7–10]. Besides, PEM fuel cells supply unregulated power [11]; however, auxiliary power electronics help to overcome this problem. According to their polarization curve, fuel cell stacks can work at different operating points characterized by the achieved voltage and current values. Then, connecting a fuel cell stack to a DC load working at a constant voltage requires a power conversion stage. A combination of a fuel cell stack and a DC/DC converter shall be known as a Regulated Fuel Cell System (RFCS) hereafter (see Fig. 1).

Fuel cell applications can be classified as stationary, telecommunications, transport or micropower. Then, stationary applications can be connected to the electric grid [12], installed as grid-independent generators [13], or operate at landfills and wastewater treatment plants [14]. Regarding telecommunication applications, fuel cells replace batteries to provide telecom sites with 1-to-5-kW power with no noise or emissions, and higher durability [15]. In transport applications, most automotive manufacturers have a fuel cell vehicle (scooter, car, bus or truck) in either developmental or testing stages [16,17]. Special attention can be paid to power in longway trucks,

* Corresponding author. Tel.: +34 959217385; fax: +34 959217348.
E-mail address: francisca.segura@diesia.uhu.es (F. Segura).

0960-1481/$ – see front matter © 2011 Elsevier Ltd. All rights reserved.
doi:10.1016/j.renene.2011.04.005

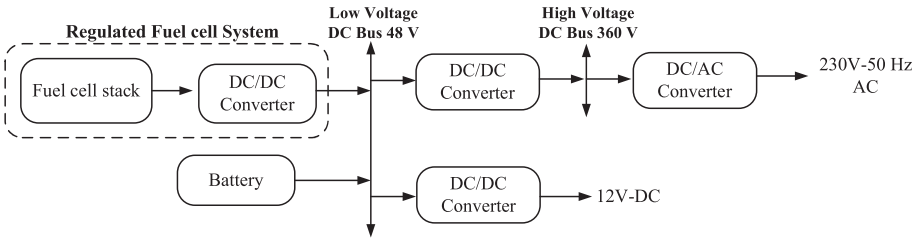

Fig. 1. Backup fuel cell stand-alone hybrid system.

commonly known as "hotel loads". The US Department of Energy (DOE) estimates that using fuel cell APUs in Class 8 trucks would save 2500 million liters of diesel fuel and 11-80 million tons of CO_2 per year [18]. On the other hand, fuel cells are currently being developed for mining locomotives, as they produce no emissions [9]. Another fuel cell application is micropower. Fuel cells will change the telecommuting world, powering cellular phones or laptops for longer hours than batteries. Companies such as Motorola, Toshiba, Samsung, Sanyo or Sony have already proved that fuel cells can power cell phones for 30 days and laptops for 20 h without recharging [19].

All these varied applications share a common basic scheme (see Fig. 2). A fuel reformer unit transforms conventional fuel into hydrogen. The fuel cell stack needs hydrogen to generate DC no-regulated electric power, and, finally, a power conditioning unit produces DC or AC regulated power. Higher system efficiency can be obtained if a co-generation system makes use of the heat generated by the fuel cell stack. This scheme can be broken down into the different topologies associated to the afore-mentioned applications.

This paper is organized as follows: Section 2 contributes a survey of topologies for fuel cell hybrid systems, while Sections 3 and 4 describe and test the real behavior of our fuel cell hybrid system according to one of these topologies. Finally, conclusions are presented in Section 5.

2. Topology survey of fuel cell hybrid systems

Power conditioning systems allow improving energy efficiency in fuel cell hybrid systems. This section aims at exploring power conditioning approaches for the afore-mentioned applications, which can be classified as follows [12]:

- Circuit topology for dedicated load supply
- Circuit topology for backup power supply
- Circuit topology for a fuel cell hybrid vehicle.

All of them comprise various power conversion blocks such as DC/DC converters and single-phase or 3-phase inverters. Since the DC voltage generated by a fuel cell stack varies widely (0–50 V for a 5–10 kW stack and 0–350 V in stacks up to 300 kW), a step-up DC/DC converter is essential to generate higher regulated DC voltage (360 V typical for 230 V–50 Hz AC output). The DC/DC converter is responsible for drawing power from the fuel cell and should therefore be designed to match fuel cell ripple current specifications.

2.1. Circuit topology for dedicated load supply

Fuel cell power conversion for a stand-alone load is a representative example of Distributed Generation (DG) [20,21]. The power conversion unit must be capable of operating within the fuel cell range and, particularly, to deliver rated power while regulating output voltage. The power conversion unit is expected to provide high quality power (THD restriction). For domestic loads, a 5:1 peak to average power capability for tripping breakers and starting motors is desired. This is an additional constraint on the design of the power conditioning unit for stand-alone loads. An auxiliary power source such as a battery or ultracapacitor bank is needed. Fig. 3 (except Buck converter and DC Load) shows the circuit topology of the power conditioning unit for this application. The DC/DC Boost converter output can be fixed, for example, at 48 V and the Push–Pull DC/DC converter output at 360 V. The single-phase inverter generates a 230 V–50 Hz AC output. A 48 V battery is connected to the DC/DC Boost converter output to provide additional power at the output terminals for start-ups and load changes. In addition, this topology is fairly common in other applications; for example:

a) *Fuel cell system to supply a load operating in parallel with the local utility* (interactive utility). In this configuration, the peak power demanded by the load is provided by the utility [22]. Paralleling the fuel cell power output to the utility offers the following advantages: 1) Power conversion rating is same as in the fuel cell; and 2) A constant fuel cell power level can be set
b) *Fuel cell system connected directly to the local utility*. Fuel cell power systems can be configured with the purpose of connecting them directly to the utility for power supply [23]. Power conversion stages must be designed according to the

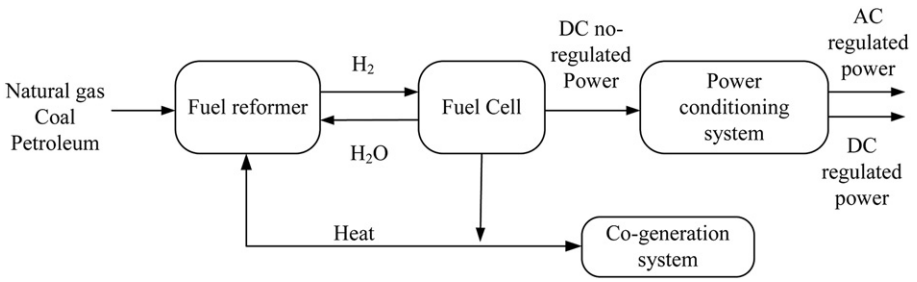

Fig. 2. Fuel cell system basic scheme.

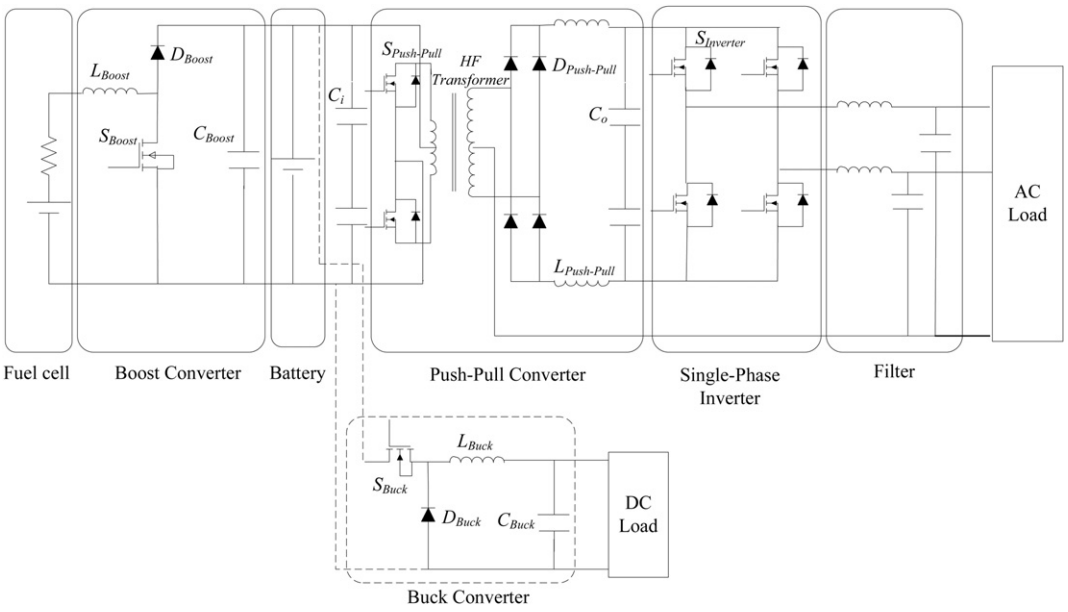

Fig. 3. Circuit topology to supply a dedicated load.

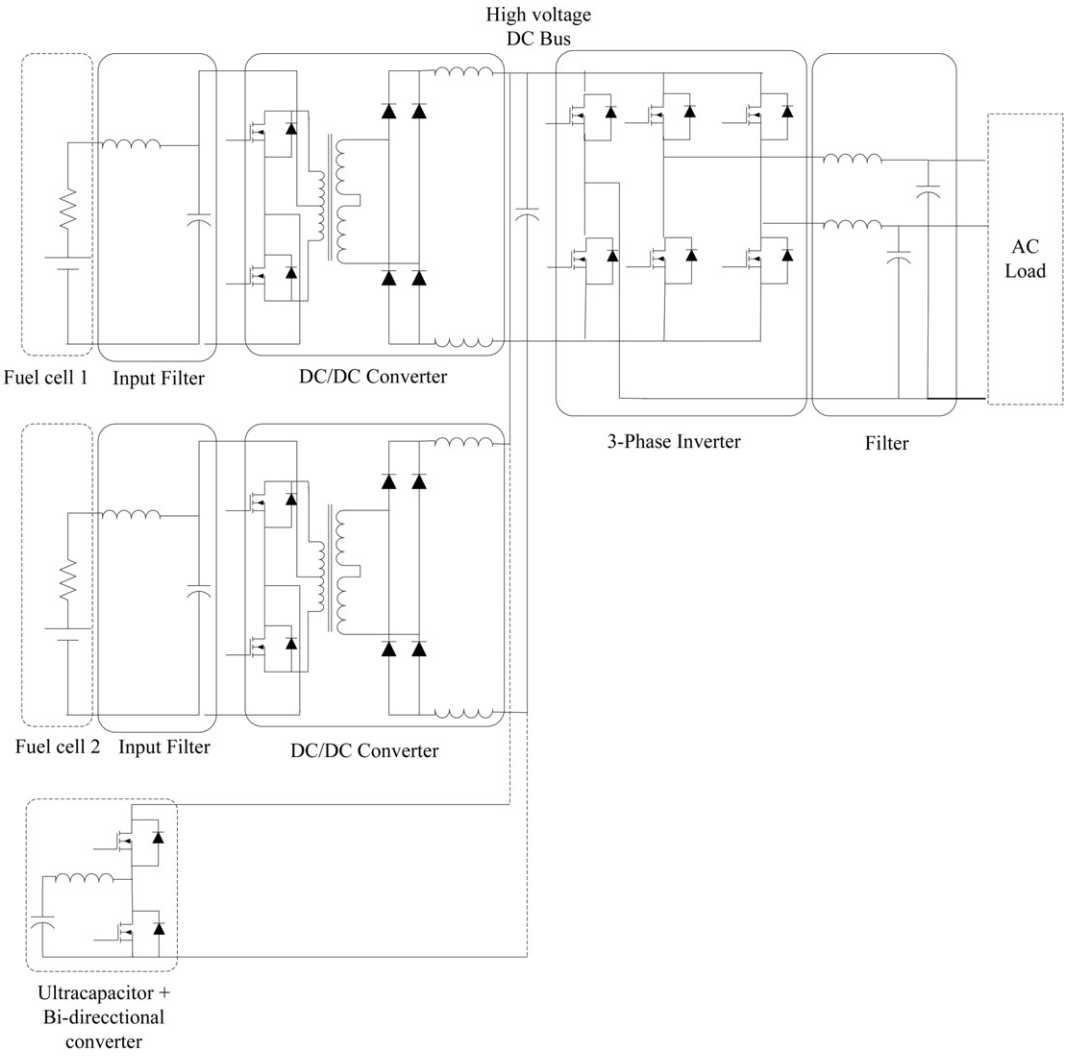

Fig. 4. Circuit topology to supply backup power.

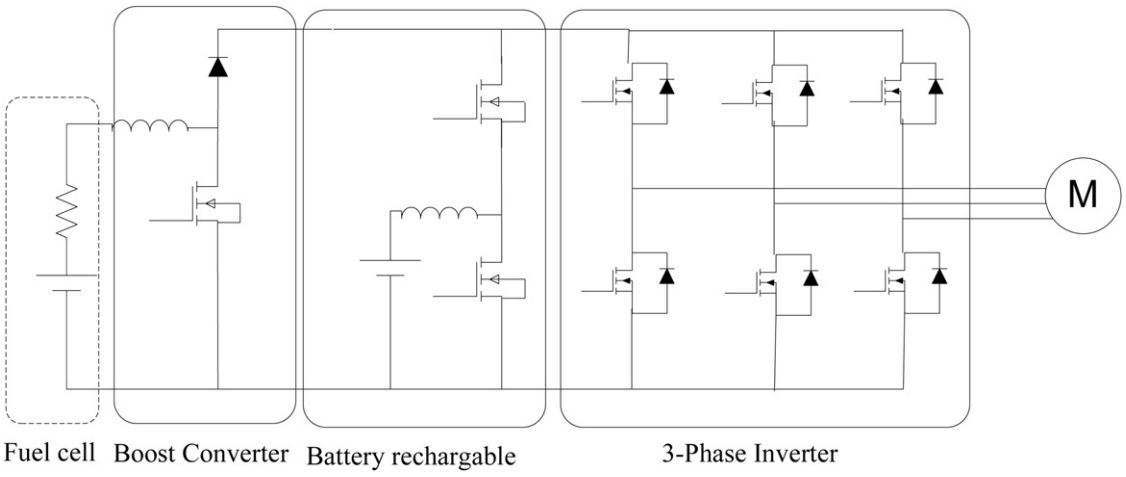

Fig. 5. Circuit topology for a fuel cell hybrid vehicle.

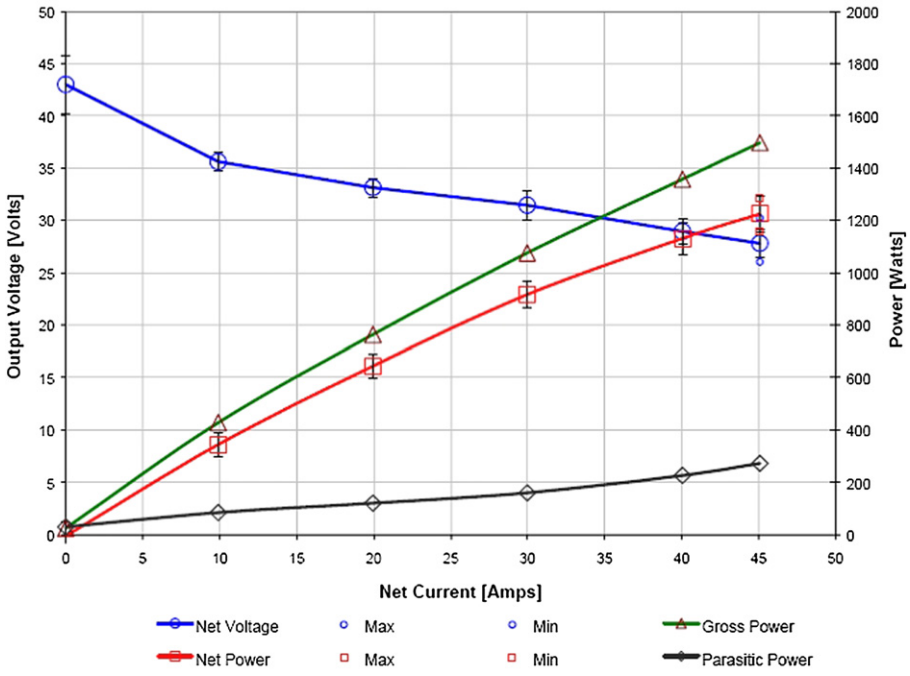

Fig. 6. Polarization and power curves for the Nexa module.

criteria and requirements for interconnecting distributed resources to the electric power system.[1]

The system built and tested in this work is based on the topology in Fig. 3. Broken lines connect the Buck converter used to transform low voltage 48 V-DC Bus into 12 V-DC output.

2.2. Circuit topology to supply backup power

A typical Uninterrupted Power System (UPS) comprises rechargeable batteries. However, these batteries contain eco-unfriendly toxic heavy metals. Furthermore, unlike batteries, fuel cells provide continuous power as long as reactants are supplied [24]. This feature is especially useful in case of uncertain power outage duration. Fig. 4 shows a scheme of a UPS mainly devoted to provide backup power to a load connected to the local utility. It uses modular DC/DC converters to interface each fuel cell output to a high voltage DC Bus. An ultracapacitor module is connected to the DC Bus through a bi-directional DC/DC converter, which allows quickly charging and discharging the ultracapacitor module to supply the load-demanded inrush current. A methodology for optimizing renewable energy size using parallel-connected DC/DC converters is presented in [25].

2.3. Circuit topology for a fuel cell hybrid vehicle

Fuel cell vehicles must achieve commercial success for the automotive fuel cell market to have direct impact on the stationary fuel cell market [26]. An effective commercialization of fuel cell

[1] Standard P1547 (US) or CENELEC EN 50160 (EU).

Table 1
Electrical characteristics for components used for Boost Converter.

Device	Type	Characteristics
Schottky Diode (D_{Boost})	MBR6045WT	2 × 45 V–60 A, 0.75 V at 25 °C
MOSFET (S_{Boost})	IRFP264	2 || 250 V–38 A, 75 mΩ
Inductance (L_{Boost})	PCV-2-568-08	6 || 568 μH, 8 A, 90 mΩ
Capacitor (C_{Boost})	MXR 160 V–2200 μF	2 || 2200 μF, 160 V

vehicles involves some requirements. Most important are the need of further development of hydrogen-reforming technologies and the availability of low cost, reliable power conditioning systems. Fig. 5 shows the typical topology of a power conditioning unit for a fuel cell hybrid vehicle powering a 3-phase variable-speed AC traction motor load.

3. Developed system description

To develop and build the system in Figs. 1 and 3, Nexa™ Power Module from Ballard and GF 12 094 Y VRLA from Exide were selected as the fuel cell stack and battery, respectively. The Nexa module was selected because it is widely well-known in fuel cells market as it is high quality, low cost, reliable and easy to use. According to the electrical features of the Nexa module [26], the highest voltage at fuel cell terminals is 43 V; a step-up converter is then necessary to connect the fuel cell stack to a low voltage 48 V-DC bus. Battery voltage is 12 V, so four batteries are connected in series to obtain 48 V. Power conditioning systems allow improved energetic efficiency in fuel cell hybrid systems. The converter sizing in topology in Figs. 1 and 3 was carried out according to the specifications of 1.5 kW rated power.

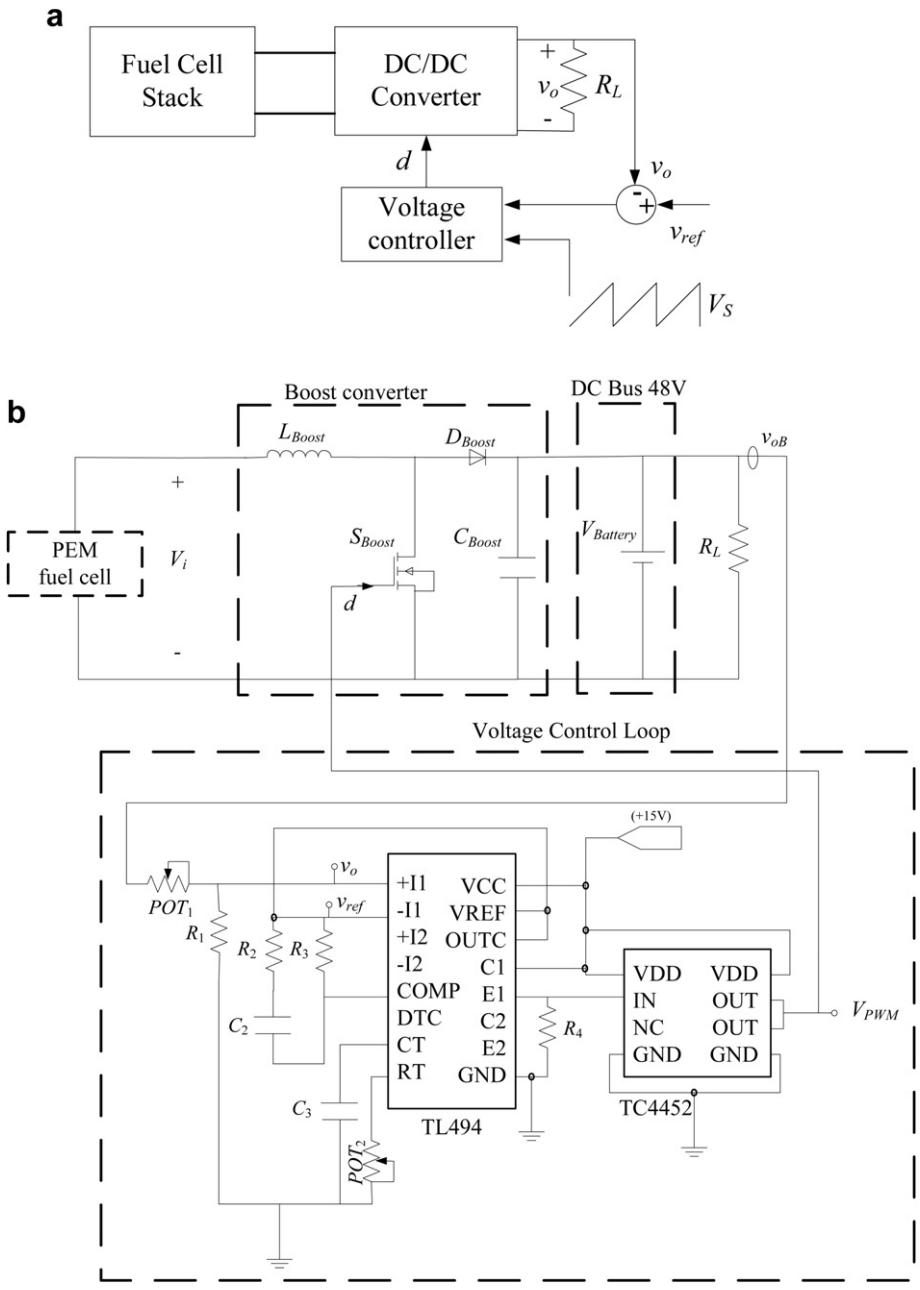

Fig. 7. a: Voltage control loop block diagram. b: Scheme of the voltage control loop applied to PEM fuel cell hybrid system.

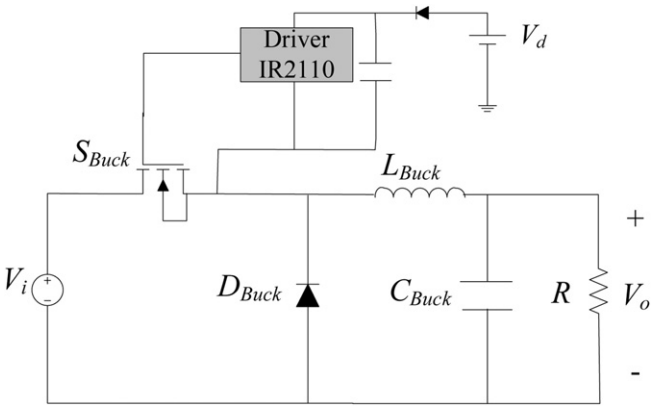

Fig. 8. Bootstrap scheme for Buck converter.

3.1. PEM fuel cell Nexa™ module

The Nexa™ Ballard Power system is capable of providing up to 1.2 kW unregulated DC power. The output voltage level can vary from 43 V at no load to about 26 V at full load (Fig. 6). Recent works [27,28] focus on a fuel cell model based on the real behavior of the Nexa module. The stack comprises 48 single cells connected in series. The operating temperature in the stack is around 65 °C at full load. 99.99% of the fuel is gas hydrogen. See Reference [26] for further details.

3.2. DC/DC Boost converter

A DC/DC step-up converter is required to connect the unregulated DC output of the fuel cell module to a low voltage 48 V-DC Bus (see Figs. 1 and 3). Since the fuel cell stack operates with a lower voltage within a wide unregulated voltage range (26–43 V), this voltage must be step-up to the regulated-voltage 48 V-DC Bus. Then, a Boost topology is selected. The electrical parameters of the components used are summarized in Table 1. Inductance and capacitance values are chosen to restrict the current and voltage ripple below 10%. The switching frequency is set to 30 kHz and the relation between inductance size and input current ripple, as well as between capacitor size and output voltage ripple are widely known; see Equations 1 and 2:

$$L_{Boost} = \frac{V_i d}{\Delta i_{L_{Boost}} f} \tag{1}$$

$$C_{Boost} = \frac{I_o d}{\Delta v_{C_{Boost}} f} \tag{2}$$

A control system was designed and built to convert the unregulated fuel cell stack output into 48 V fixed voltage (Fig. 7a). This control system is based on a pulse width modulation (PWM) control circuit (TL494). This circuit provides a PWM signal (duty cycle) to control the Boost converter and incorporates all the functions required in the construction of a PWM control circuit on a single chip. The Boost output voltage, v_{oB}, (Fig. 7b) is connected to the +I1 input through the variable voltage divider comprised by POT_1 y R_1 (the sensed signal v_o in Fig. 7a corresponds to +I1 input in Fig. 7b). The voltage divider allows varying the sensed signal within the 0–5 V interval (the voltage range that can handle the integrated circuit). The reference signal v_{ref} which represents the voltage to follow (see Fig. 7a) is connected to the −I1 input (Fig. 7b). The network integrated by R_2, R_3 and C_2 is the compensation network. C_3 and POT_2 generate the sawtooth signal V_s (see Fig. 7b). The integrated circuit TC4452 is the driver used to generate the signal, whose voltage and current levels must be high enough to drive the transistor gate.

Table 2
Electrical characteristics for components used for Buck converter.

Device	Type	Characteristics
Schottky Diode (D_{Buck})	MBR6045WT	2 × 45 V–60 A, 0.75 V at 25 °C
MOSFET (S_{Buck})	IRFP264	250 V–38 A, 75 mΩ
Inductance (L_{Buck})	PCV-2-568-08	5 || 568 μH, 8 A, 90 mΩ
Capacitor (C_{Buck})	YXF 63 V–1000 μF	2 || 1000 μF, 63 V

Table 3
Electrical characteristics for components used for Push–Pull converter.

Device	Type	Characteristics
HF transformer	Ferrite Core E6527	Primary: 8T C.T. 4//#16 AWG Secondary: 64T C.T. 2//#20 AWG
Toroidal inductor ($L_{Push-Pull}$)	ITL500	2 × 500 μH, 21,76 A, 20 mΩ
MOSFET ($S_{Push-Pull}$)	IRFP264 4	4 || 250 V–38 A, 75 mΩ
Fast recovery rectifier ($D_{Push-Pull}$)	BYT60P1000	2 × 1000 V–60 A, 1.8 V
C_{input} (C_i)	MXR	2 × 470 μF, 160 V
C_{output} (C_o)	MXR	2 × 470 μF, 470 V

3.3. DC/DC step-down converter

A DC/DC step-down converter is required to convert the regulated 48 V-DC Bus into regulated 12 V-DC output. The Buck converter has the simplest topology and the lowest number of components [29]. For DC output voltage control, it includes a similar loop to that in the Boost converter. In the Buck converter, the reference node for the gate drive is not a constant voltage and must refer to a floating point, as the MOSFET source terminal is not connected to a negative low voltage DC Bus (Fig. 8). Then, conventional bootstrap structure was used. The components' electrical parameters are summarized in Table 2. Inductance and capacitance values are chosen to keep the current and voltage ripple below 10%. The switching frequency is fixed to 30 kHz and the relation between inductance size and input current ripple, as well as between capacitor size and output voltage ripple are known; see Equations 3 and 4:

$$L_{Buck} = \frac{(V_i - V_o)d}{\Delta i_{L_{Buck}} f} \tag{3}$$

$$C_{Buck} = \frac{V_o(1-d)}{8L_{Buck}\Delta v_o f^2} \tag{4}$$

3.4. Push–Pull converter

When a large step-up conversion ratio is required, an isolated DC/DC converter is preferred. The galvanic insulation between the low voltage DC Bus 48 V and the high voltage DC Bus 360 V is obtained with a high frequency (HF) transformer.

Table 4
Electrical characteristics for components used for Single-phase inverter.

Device		Type	Characteristics
Controller	Digital signal controller	dsPIC30F2010	28-Pin 16-Bit enhanced flash
	Gate driver	IR2110	Bootstrap operation, 10 ns delay, ton/off 120 ns
	Gate optocoupler	HCPL2231	8-Pin DIP, 300 ns propagation delay
IGBT ($S_{Inverter}$)		HGTG40N60	4 × 600 V, 70 A, 1.5 V at 150 °C

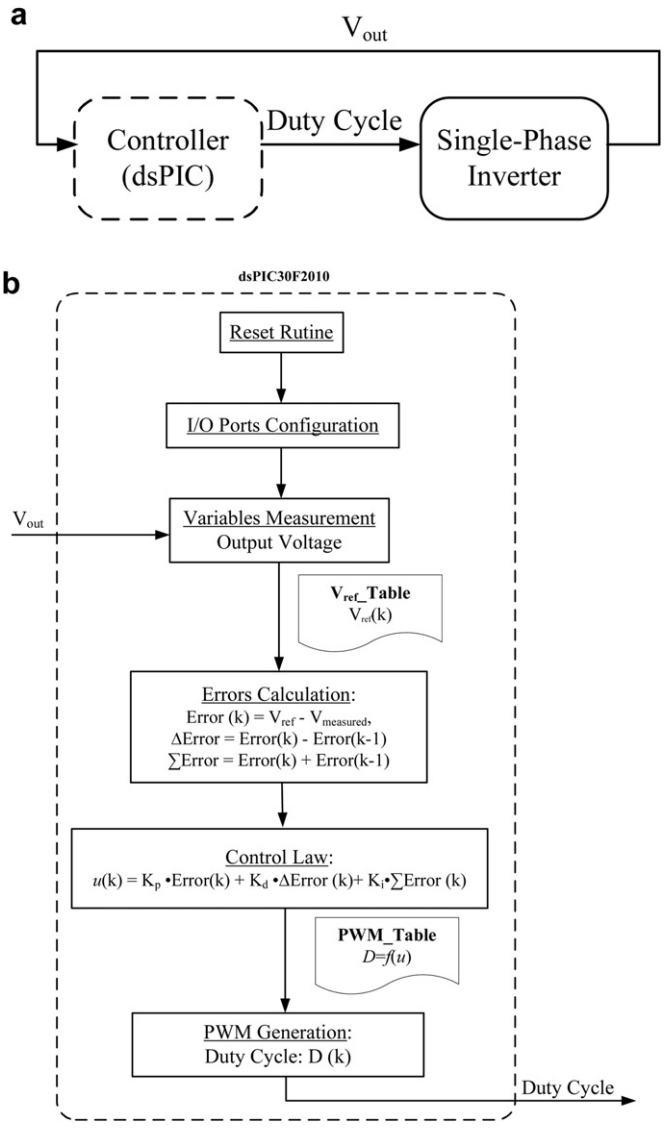

Fig. 9. a: Inverter control scheme implemented. b: Inverter control on dsPIC30F2010.

These are the main reasons that led us to choose Push–Pull converter to co-operate with fuel cell: 1) Insulation, as the Push–Pull converter includes a reduced-size-and-weight high frequency (HF) transformer; 2) the Push–Pull converter is widely used in low-input voltage applications. In this case, voltage level at the Push–Pull input terminal is 48 V (fixed by the Boost converter),

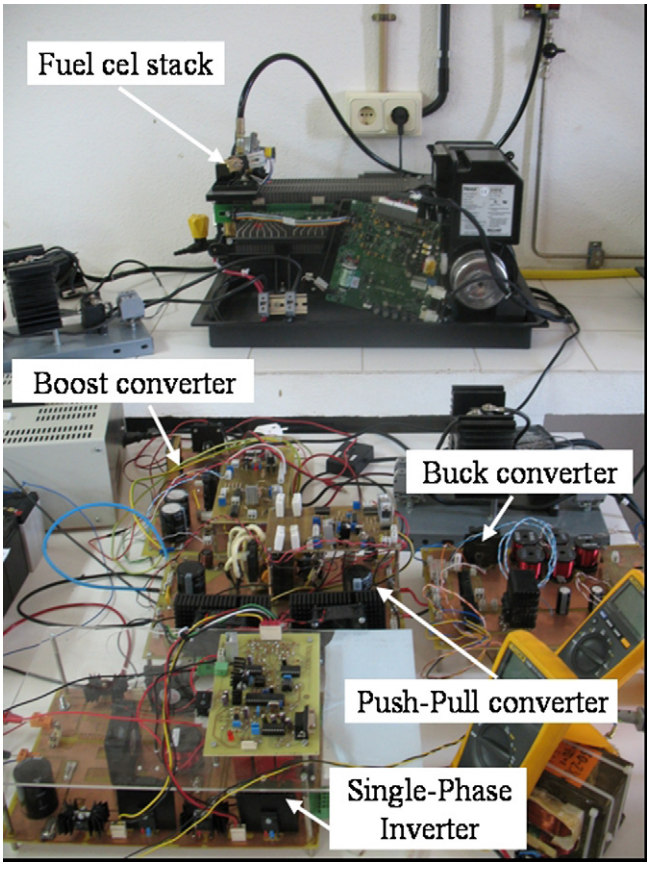

Fig. 11. Distributed generation system with fuel cell developed.

whereas output voltage is 360 V, almost an order of magnitude higher; and 3) the Push–Pull converter has only two power switches whose control voltages share the same reference, so the control circuit is thus easier than other isolated converters.

The Push–Pull topology with a full-wave center-tapped rectifier on secondary is selected to reduce conduction losses in the switches. Thus, the Push–Pull DC/DC converter is the most competitive solution for low-input voltage applications. The switching power devices used in the converter topology can be either Insulated Gate Bipolar Transistors (IGBTs) or MOSFETs. For high power applications and fuel cell output voltage over 150 V, the IGBT can be used as a power device. In spite of its lower on-state voltage drop, higher power density and lower cost when compared to the MOSFET, the IGBT has higher switching losses and limited switching frequency. In particular, the turn-off switching loss is very high because of the IGBT

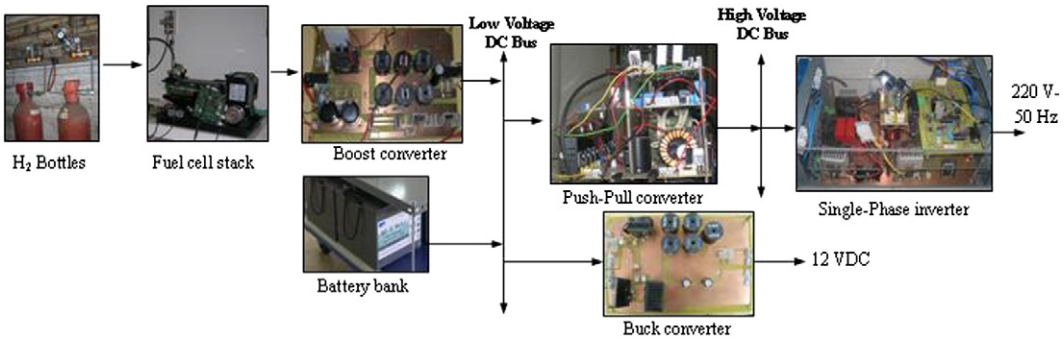

Fig. 10. Simplified scheme with actual systems of the distributed generation system with fuel cell developed.

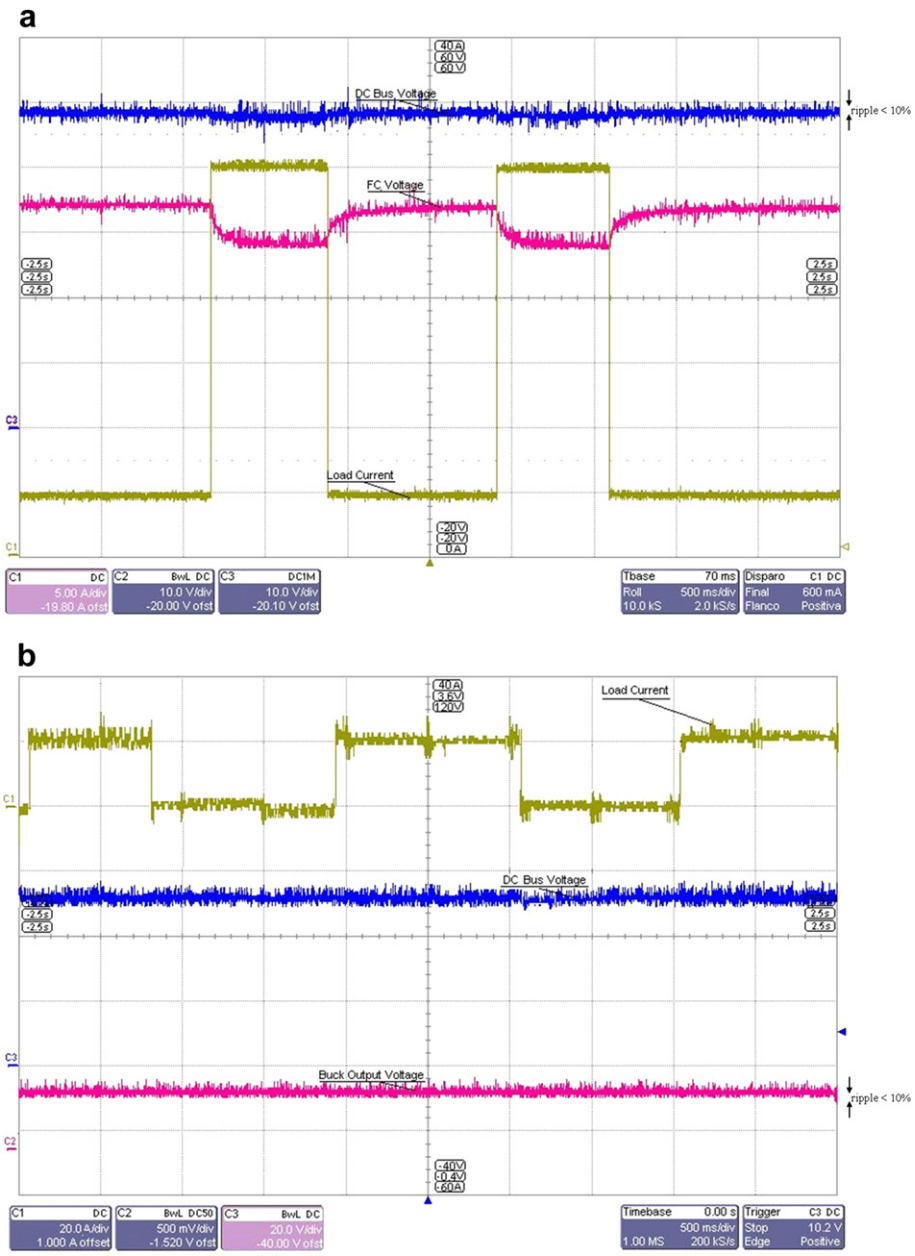

Fig. 12. Experimental results when load is connected to DC links. a) Load connected to Low Voltage DC Bus: Load current (Channel C1: 5 A/div, 500 ms/div), Fuel cell voltage (Channel C2: 10 V/div, 500 ms/div), Low DC Bus voltage (Channel C3: 10 V/div, 500 ms/div). b) Load connected to 12 VDC output: Load current (Channel C1: 20 A/div, 500 ms/div), Buck output voltage (Channel C2: 500 mV/div, 500 ms/div, probex20), Low DC Bus voltage (Channel C3: 20 V/div, 500 ms/div).

current-tail phenomena. The size and weight of DC/DC converter reactive elements (HF transformer and *LC* filter) can be reduced by increasing the switching frequency, but the switching power losses will proportionally increase with the frequency. Therefore, it requires a commitment to the switching frequency, which was set to 30 kHz. A SG3825 PWM controller is used as a part of the voltage-fed Push–Pull DC/DC converter control circuitry due to its integrated drive protection and low cost. The SG3825 is optimized for high frequency switched mode power supply applications. Particular care was paid to minimizing propagation delays through the comparators and logic circuitry while maximizing bandwidth and the slew rate of the error amplifier. This controller was designed to be used in either current mode or voltage mode systems with capability for input voltage feedforward. Protection circuitry includes a current limit comparator with a 1 V threshold, a TTL compatible shutdown port, and a soft start pin which will also operate as a maximum duty cycle clamp. The logic is fully latched to provide jitter free operation and prevent multiple pulses at an output. This device features totem pole outputs designed to source and sink high peak currents from capacitive loads, such as the gate of a power MOSFET. A HF transformer with 1:8 turn ratio was designed for this purpose. The components' descriptions are summarized in Table 3.

3.5. Single-phase inverter

The input to the inverter is the free running chopper rectified square wave. After appropriate DC Bus filtering, this waveform is fed into the single-phase inverter circuit (Figs. 1 and 3). A standard H-bridge inverter is selected due appropriate use and high efficiency capability. The H-Bridge is controlled by a digital signal controller running at 25 MHz. Its output (differentially) consists on a waveform of rectangular pulses with a 20-kHz constant frequency and a duty

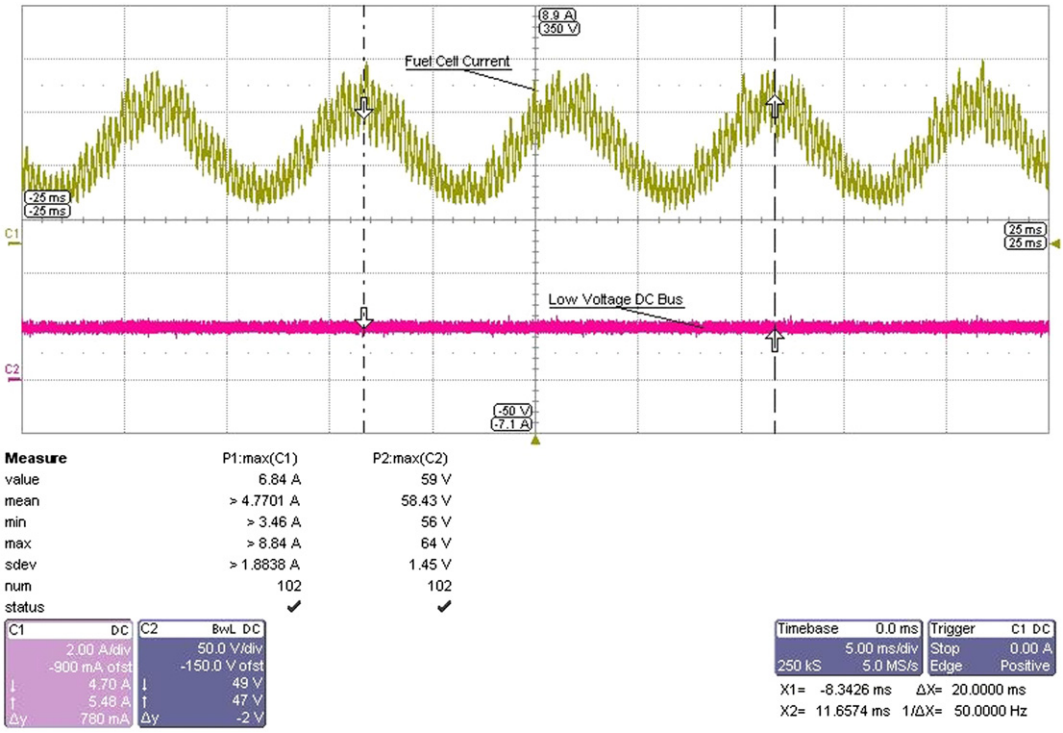

Fig. 13. Experimental results when load is connected to AC Output. Fuel cell current (Channel C1: 2 A/div, 5 ms/div), 48 V-DC Bus voltage (Channel C2: 50 V/div, 5 ms/div).

cycle that varies to correspond with the absolute value of the desired output sine wave. The high side switches of the H-Bridge switch at high frequency (20 kHz), while low side ones switch at low frequency (50 Hz) The output filtering provides the smooth sine wave. A low-pass LC filter eliminates ripple from the output voltage.

The control scheme is implemented in a cost-effective digital signal controller dsPIC30F2010, which generates the PWM signal to set the H-bridge switching frequency. The dsPIC30F2010 controls both the inverter through the hardware protection circuitry and H-Bridge drivers. IGBTs are used for the H-Bridge rather than MOSFETs due to their lower on-resistance. Although IGBTs have a slower turn on time than MOSFETs, their relatively low operation frequency (20 kHz) makes this property irrelevant. The components' electrical parameters are summarized in Table 4. In this case, the controller parameters are modified according to the process operating conditions [30]. The single-phase inverter operating conditions are defined by the output voltage (Fig. 9a). Then, the error value can be calculated by subtracting the reference value to the measured value (Fig. 9b). "V_{ref}_Table" provides the reference value according to the operating point. Moreover, error addition and subtraction can be

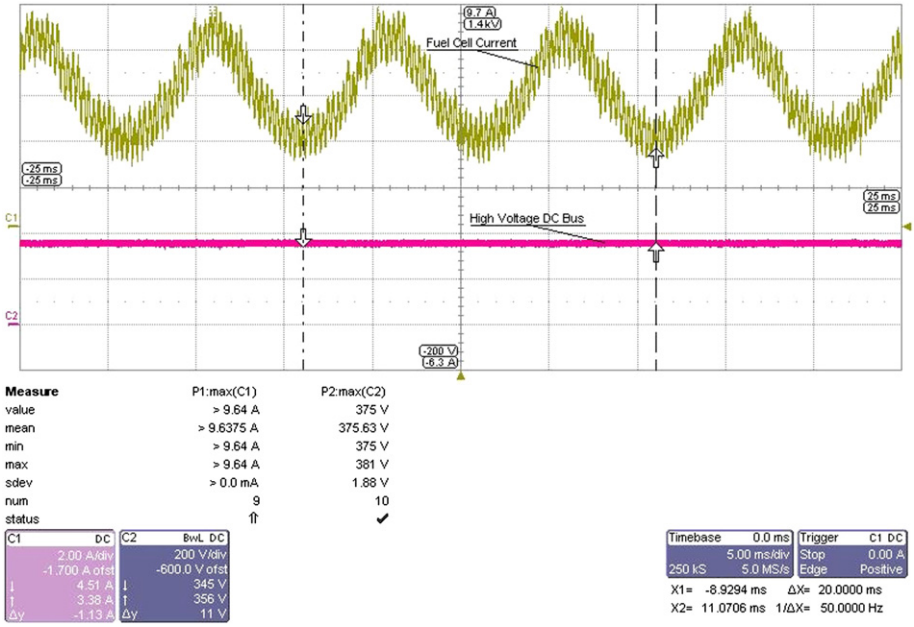

Fig. 14. Experimental results when load is connected to AC Output. Fuel cell current (Channel C1: 2 A/div, 5 ms/div), 360 V-DC Bus voltage (Channel C2: 200 V/div, 5 ms/div).

obtained. Then, the control action is worked out according to the product of proportional, integral and derivative constants and errors, respectively. PWM_Table allows generating the duty cycle for transistor switching. The microcontroller is programmed with a sequence of sentences and tables, so output voltage and duty cycle are input and output, respectively. Sample rate is 50 μs.

When the load is connected to the single-phase inverter, generation and propagation of low frequency (100 Hz) current ripple up to fuel cell stack is expected [31]. This low frequency current ripple can be explained by the energy conservation law assuming linear load. The voltage and current of the inverter output (v_o, i_o) are expressed in Equations 5 and 6:

$$v_o(t) = V_m \cos(\omega t + \theta) \tag{5}$$

$$i_o(t) = I_m \cos(\omega t + \phi) \tag{6}$$

where V_m and I_m are voltage and current amplitude, and θ and ϕ stand for phase angles.

The frequencies of the output voltage and current are the same as ω, so the frequency of the inverter output power (P_o) doubles (2ω) it. This can be derived as from Equation (7):

$$P_o(t) = \frac{V_m I_m}{2}(\cos(2\omega t + \theta + \phi) + \cos(\theta - \phi)) \tag{7}$$

Power at output inverter, DC links (low and high voltage) and fuel cell terminals should be identical by means of the energy conservation law as shown in Equation (8), neglecting converter and inverter loss:

$$P_o(t) = P_{DCBus}(t) = P_{FC}(t) \tag{8}$$

The frequency and shape of the low voltage DC Bus current (i_{DCBus}) is the same as the inverter output power and can be calculated as in (9), because DC Bus voltage is regulated by controlling converter output voltage.

$$i_{DCBus}(t) = \frac{V_m I_m}{2V_{DCBus}}(\cos(2\omega t + \theta + \phi) + \cos(\theta - \phi)) \tag{9}$$

According to Equation (9), DC Bus current waveform is modulated by two frequencies: the switching frequency itself (30 kHz) and the 100 Hz (2·50 Hz) frequency derived from the AC output. Then, according to Figs. 1 and 3, the fuel cell current shows the 100 Hz ripple on top of the pulsating DC current due to the switching behavior of single-phase inverter when non-linearity and fuel cell dynamics are neglected.

4. Experimental results

The aim of this work is not to proposing a new energy management but focusing on proving that specific voltage levels can be achieved at interconnecting points. Experimental results are divided into three cases. The first consists on connecting a load to a low voltage DC Bus, where both fuel cell stack and battery bank work together, while the second consists on connecting the load to a 12 V-DC output. In this case, the aim is guaranteeing the low voltage DC Bus (48 V) and DC output voltage (12 V) over the whole Buck converter operating range. Finally, the last results correspond to connecting the load to an AC output. Results show the waveform at the AC output, high voltage at the DC Bus and low voltage at the DC Bus. Experimental results were obtained with a LeCroy 500 MHz oscilloscope. Figs. 10 and 11 show a scheme with actual photographs of the whole system.

4.1. Load connected to a low voltage 48 V-DC bus (Fig. 12a)

In this case, both fuel cell system and battery bank are supplying power to a low voltage DC Bus. Subsequently, when the load demands a step power varying from 240 W to 1.5 kW, the following can be observed:

a) At low power (240 W), load current is 5 A, low bus voltage is set to 48 V and fuel cell module voltage is 35 V. Then, with the help of polarization and power curves (Fig. 6), the fuel cell operating point is known (35 V, 7 A, 245 W) and the fuel cell stack can be concluded to be the only source supplying power to the load

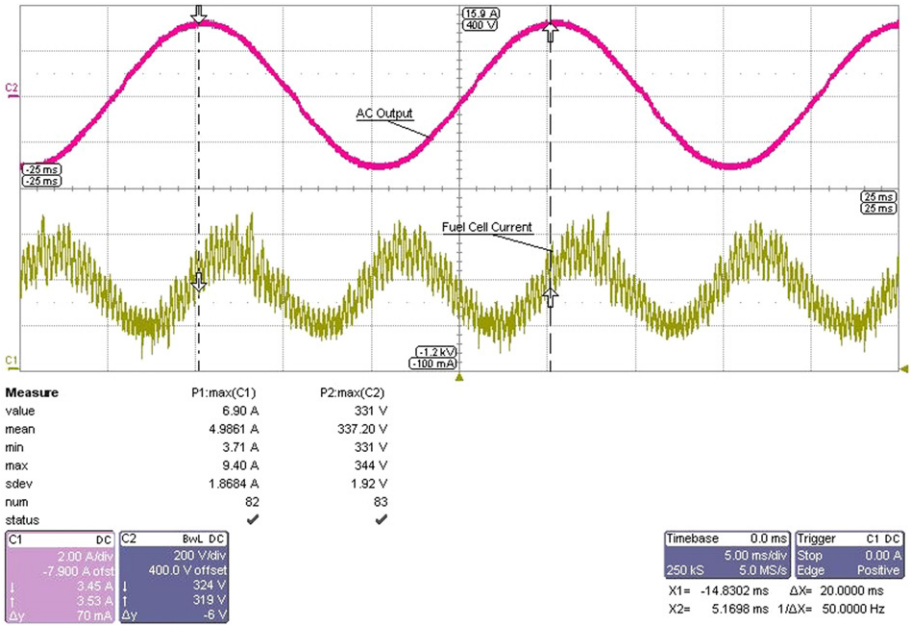

Fig. 15. Experimental results when load is connected to AC Output. Fuel cell current (Channel C1: 2 A/div, 5 ms/div), 230 V-AC Single-phase inverter output voltage (Channel C2: 200 V/div, 5 ms/div).

b) At high power (1.5 kW), load current is 30 A, low DC Bus voltage is set to 48 V and fuel cell voltage is 28 V. Then, according to Fig. 6, fuel cell stack works at rated power (1.2 kW). The battery bank supplies the difference between load power and fuel cell rated power. Moreover, the slow fuel cell response can be observed in Fig. 12a when a step load happens. This is the main reason to use an auxiliary power source when a fuel cell stack supplies a variable load.

4.2. Load connected to a Buck converter (Fig. 12b)

In this case, the load is connected to a low voltage DC output (12 V). Because of low output voltage value and to handle secure current levels, test is carried out supplying 240 W rated power. Load current demand will be 20 A and the voltage control board must adjust the Buck converter's duty cycle to keep output voltage at 12 V. In this case, the theoretical output current fits in the experimental value. Fig. 12b shows the load current (output current) and voltage at the Buck input and output terminals. The input voltage (low voltage DC Bus) is set to 48 V and DC output voltage is regulated to 12 V-DC even when load power demand reaches the highest value. The load power demand in this last test was so low that the fuel cell system is the only working source.

In these two cases (a load connected to a 48 V-DC bus and a load connected to a 12 V-DC output), the switching frequency is responsible for high frequency voltage and current ripple, and this ripple is kept below the design's parameters.

4.3. Load connected to a single-phase inverter (Figs. 13, 14 and 15)

In this case, the load was connected to an AC output. Results show the waveform at a low voltage 48 V-DC Bus (Fig. 13), high voltage 360 V-DC Bus (Fig. 14), inverter AC output voltage (Fig. 15) and fuel cell current. A 230 V–50 Hz signal can be observed at AC output while voltage at low and high DC Bus is set to 48 and 360 V, respectively, when the load is connected to inverter terminals. Moreover, as mentioned in Section 3, low frequency current ripple (100 Hz) can be observed to be over high frequency ripple when compared to the 50 Hz-AC output.

5. Conclusions

The designed system is an excellent testing bench where power electronics plays an essential role. The performance of a fuel cell hybrid system can be tested at different voltage-restricted interconnecting points; as well as the performance of different power sources and a system under different load profiles. Moreover, versatility and structural simplicity are some its main advantages.

This is a solution to a practical case related to a distributed generation fuel cell hybrid system. The main restriction in the design process is the availability of commercial components. This system comprises a fuel cell module, a battery bank, 4 power converters and all associated electronics.

This system includes 4 main interconnecting points (48, 360, 12 and 230 V-AC), which give rise to greater restrictions and the cascade connection between different stages demands special attention.

Experimental results show that the whole system works in a suitable way when different load power values are demanded by a low voltage 48 V-DC Bus (fuel cell system works simultaneously with battery bank) and 12 V-DC and AC outputs. Moreover, voltage levels in different electrical interconnection points were proven to have been achieved (48 and 12 V-DC and 230 V-AC) even when load demands high power values. Finally, high and low frequency fuel cell current ripples were also shown.

Acknowledgments

This work is a contribution of the DPI2010-17123 Project supported in part by the Spanish Ministry of Education and Science and in part by the European Regional Development Union.

References

[1] Obara S. Power characteristics of a fuel cell micro-grid with wind power generation. International Journal of Energy Research 2007;31:1064–75.
[2] Babu CA, Ashok S. Optimal utilization of renewable energy-based IPPs for industrial load management. Renewable Energy 2009;34:2455–60.
[3] Tsoutsos T, Papadopoulou E, Katsiri A, Papadopoulos AM. Supporting schemes for renewable energy sources and their impact on reducing the emissions of greenhouse gases in Greece. Renewable and Sustainable Energy Reviews 2008;12:1767–88.
[4] Yan X, Crookes RJ. Life cycle analysis of energy use and greenhouse gas emissions for road transportation fuels in China. Renewable and Sustainable Energy Reviews 2009;13:2505–14.
[5] Segura F, Andújar JM, Tomé JM. "Solutions to power management based on voltage and current control methods applied to fuel cell hybrid systems", regular-paper accepted for Biogreen-2010 (http://www.iaria.org/conferences2010/CfPBIOGREEN10.html).
[6] Thounthong P, Rael S, Davat B. Energy management of fuel cell/battery/supercapacitor hybrid power source for vehicle applications. Journal of Power Sources 2009;193:376–85.
[7] Düsterwald HG, Günnewig J, Radtke P. DRIVE - The future of automotive power: fuel cells perspective. Fuel Cells 2007;7:183–9.
[8] Tao Haimin, Duarte JL, Hendrix MAM. Line-interactive UPS using a fuel cell as the primary source. IEEE Trans. on Industrial Electronics 2008;55:3012–21.
[9] Miller AR, Hess KS, Barnes DL, Erickson TL. System design of a large fuel cell hybrid locomotive. Journal of Power Sources 2007;173:935–42.
[10] Segura F, Durán E, Andújar JM. Design, building and testing of a stand alone fuel cell hybrid system. Journal of Power Sources 2009;193(1):276–84.
[11] Moreira MV, da Silva GE. A practical model for evaluating the performance of proton exchange membrane fuel cells. Renewable Energy 2009;34:1734–41.
[12] Kirubakaran A, Jain S, Nema RK. A review on fuel cell technologies and power electronic interface. Renewable and Sustainable Energy Reviews 2009;13:2430–40.
[13] Paska J, Biczel P, Kłos M. Hybrid power systems – An effective way of utilising primary energy sources. Renewable Energy 2009;34:2414–21.
[14] Osorio F, Torres JC. Biogas purification from anaerobic digestion in a wastewater treatment plant for biofuel production. Renewable Energy 2009;34:2164–71.
[15] Gianolio G, Rosso I, Mercante L, Pedrazzo F, Simonato G, Ceriani F. Green-Shelter for telecom applications: a new generation of shelters for telecom applications integrating fuel cell electric backup and a new cooling approach. IEEE International Telecommunications Energy Conference (Proceedings on INTELEC); 2008. art. n. 4664059.
[16] Andújar JM, Segura F. Fuel cells: history and updating. A walk along two centuries. Renewable and Sustainable Energy Reviews 2009;13:2309–22.
[17] Intelligent energy launches first fuel cell motorbike. Fuel Cells Bulletin 2005;1(4).1.
[18] Second US Army truck with fuel cell APU". Fuel Cells Bulletin 2003;1(4).
[19] Ross D. Power struggle. IEE Review 2003;49:34–8.
[20] Wang Y, Choi S, Lee E. Fuel cell power conditioning system design for residential application. Journal of Hydrogen Energy 2009;34:2340–9.
[21] Segura F, Andújar JM, Durán E. Design, building and testing of a stand alone fuel cell hybrid system. Journal of Power Sources 2009;193:276–84.
[22] Zhan Yuedong, Guo Youguang, Zhu Jianguo, Wang Hua. Intelligent uninterruptible power supply system with back-up fuel cell/battery hybrid power source. Journal of Power Sources 2008;179:745–53.
[23] Kanase-Patil AB, Saini RP, Sharma MP. Integrated renewable energy systems for off grid rural electrification of remote area. Renewable Energy 2010;35:1342–9.
[24] Scrivano G, Piacentino A, Cardona F. Experimental characterization of PEM fuel cells by micro-models for the prediction of on-site performance. Renewable Energy 2009;34:634–9.
[25] Vasallo MJ, Andújar JM, Segura F. A methodology for optimizing stand-alone PV-system size using parallel-connected DC/DC converters. IEEE Trans. on Industrial Electronics 2008;55:2664–73.
[26] Lagorse J, Paire D, Miraoui A. Sizing optimization of a stand-alone street lighting system powered by a hybrid system using fuel cell, PV and battery. Renewable Energy 2009;34:683–91.

[27] Andújar JM, Segura F, Vasallo MJ. A suitable model plant for control of the set fuel cell-DC/DC converter. Renewable Energy 2008;33:813–26.
[28] Ali DM. IEEE Power System Conference; 2008. 480.
[29] Durán E, Galán J, Sidrach-de-Cardona M, Andújar JM. A new application of the buck-boostderived converters to obtain the I–V curve of photovoltaic modules. PESC Record – IEEE Annual Power Electronics Specialists Conference, art. no. 4342022 2007, pp. 413–417.
[30] Bolat ED, Erkan K, Postalcloglu S. Using current mode fuzzy gain scheduling of PI controller for UPS inverter, IEEE Conference on Computer as a Tool, 2; 2005, 1505–1508.
[31] Kim Jong-Soo, Kang Hyun-Soo, Lee Byoung-Kuk, Lee Won-Yong. Analysis of low frequency current ripples of fuel cell systems based on a residential loads modelling. IEEE Proceeding of International Conference on Electrical Machines and Systems (ICEMS); 2007:282–7.